Glycoconj J (2007) 24:167–180
DOI 10.1007/s10719-006-9025-9

Chemical validation of molecular mimicry: interaction of cholera toxin with *Campylobacter* lipooligosaccharides

Seigo Usuki · Mohanasundari Pajaniappan · Stuart A. Thompson · Robert K. Yu

Received: 7 October 2006 / Revised: 14 November 2006 / Accepted: 20 November 2006 / Published online: 17 January 2007

Abstract It is generally believed that molecular mimicry between bacterial lipooligosaccharide (LOS) and nerve glycolipids may play an important pathogenic role in immune-mediated peripheral neuropathy. One of the putative infectious agents is *Campylobacter jejuni* (*C. jejuni*). To elucidate the structural basis for the molecular mimicry, we investigated the structure of the lipooligosaccharide (LOS) fraction of *C. jejuni*, strain HS19, and found that it includes at least two components, characterized as fast-and slow-moving bands (LF and LS) by thin-layer chromatography as revealed by cholera toxin B subunit (Ctxb) overlay. Structural analysis of the oligosaccharide portion of LS established that it had the following structure: Gal-GalNAc-(NeuAc)Gal-Hep-(Glc;PO_3H)Hep-Kdo. The GM1-like epitope was validated by a terminal tetrasaccharide unit within this structure. On the other hand, analysis of LF revealed an entirely different structure: 1, 4′-bisphosphoryl glucosamine disaccharide *N, N'*-acylated by 3-(2-hydroxytetracosanoyloxy)octadecanoic acid at 2- and 2′-positions, which is consistent with that of lipid A. No GM1-like epitope was observed in LF. Both LS and LF interacted with Ctxb as demonstrated by TLC-overlay and sucrose density gradient centrifugation. Surprisingly, LF does not have the basic GM1 structure for interacting with Ctxb. Instead, the affinity of LF to Ctxb required that one or both of the phosphate groups be present in the glucosamine disaccharide residue because after alkaline phosphatase treatment the dephosphorylated LF was unable to bind to Ctxb. We conclude that LS is likely the component contributing to GM1-mimicry in autoimmune peripheral neuropathy and that the role of LF is not clear but may be associated with the initial activation of autoreactive *T* cells.

Keywords Ganglioside · *Campylobacter jejuni* · Cholera toxin · GM1 · Molecular mimicry

Abbreviations

LOS	lipooligosaccharide
LPS	lipopolysaccharide
Ctxb	Cholera toxin B subunit
C. jejuni	*Campylobacter jejuni*
ABOE	*p*-aminobenzoic acid octyl ester
ABEE	*p*-aminobenzoic acid ethyl ester
DMB	1, 2-diamino-4, 5-methylenedioxybenzene dihydrochloride
MALDI-TOF	matrix-assisted laser desorption ionization time-of-flight
Glc	glucose
Gal	Galactose
Hep	L-*glycero*-D-*manno*-heptose
GalNAc	*N*-acetylgalactosamine
NeuAc	*N*-acetylneuraminic acid
Kdo	2-keto-3-deoxyoctanoate
BSA	Bovine serum albumin
HPTLC	High-performance thin-layer chromatography

Introduction

Elevation of serum antibody titers against GM1 ganglioside has frequently been characterized as a representative event

Ganglioside nomenclature is based on that of Svennerholm [50]

S. Usuki · R. K. Yu (✉)
Institute of Molecular Medicine and Genetics
and Institute of Neuroscience,
Medical College of Georgia,
Augusta, GA 30912-2697, USA
e-mail: ryu@mcg.edu

M. Pajaniappan · S. A. Thompson
Department of Biochemistry and Molecular Biology,
Medical College of Georgia,
Augusta, GA 30912, USA

of Guillain-Barré syndrome (GBS)[1–3]. Although the etiological mechanism for generating anti-GM1 antibodies has not been fully clarified, Campylobacteriosis is a potential risk factor for GBS, causing the production of high-titer anti-GM1 antibodies [4–6]. *Campylobacter jejuni* (*C. jejuni*) is a gram-negative bacterium expressing two components of strain-specific lipooligosaccharides (LOSs), a lipid A (or endotoxin) portion and a polysaccharide portion [7, 8]. Molecular mimicry between the carbohydrate structures of GM1 and of LOS derived from the serotype HS19 of *C. jejuni* is presumed to be a trigger for antibody production [9, 10]. We found that the LOS from strain HS19 of *C. jejuni* was composed of two distinct components distinguishable by the TLC-overlay profile to cholera toxin binding; these components are provisionally designated as fast- and slow-moving bands (LF and LS) based on their mobility on the TLC plate.

Cholera toxin is a hexameric bacterial toxin composed of a monomeric A subunit and a pentameric B subunit. The cholera toxin B subunit (Ctxb) possesses binding activity to GM1 by recognizing a specific epitope of the oligosaccharide portion of the GMl molecule. Binding of Ctxb with its ligand is not limited to GM1; several other glycosphingolipids (GSLs) also bind to Ctxb with less avidity (1- to 90-fold) to GM1 in the following order: GM1>GM1-Fuc>>GM2>GD1a>GM3>GT1b>GD1b>asialo GM1 [11]. It is interesting to note that binding of Ctxb is not limited to GSLs. Recently, it has been reported that polyphenols also possess binding affinity to Ctxb to form a Ctxb-polyphenol complex, though their dissociation constants have not yet compared with those of GM1 [12]. For this reason other non-GSL components that bind Ctxb should be carefully validated by chemical analysis. In consideration of the Ctxb-binding components of the LOS fraction, we hypothesized that molecular mimicry of the carbohydrate structure with GM1 is present in these components. We purified two components, LS and LF, and analyzed their chemical structures. We report here that LS is characterized as an octasaccharide containing a GM1-like component and LF is lipid A containing long-chain fatty acids. Both structures react with Ctxb owing to completely different mechanisms.

Materials and methods

Materials

The following items were purchased: high-performance thin-layer chromatography (HPTLC) plates coated with silica gel 60 (aluminum-backed sheets) from E. Merck, Darmstadt, Germany; o-phenylenediamine dihydrochloride tablet set (OPD Peroxidase Substrate), biotin-labeled cholera toxin B subunit, horseradish peroxidase-labeled cholera toxin B subunit, p-aminobenzoic acid ethyl ester (ABEE), diphosphoryl lipid A (from *Escherichia coli* F583, Rd mutant), monophosphoryl lipid A (from *E. coli* F583, Rd mutant), and alkaline phosphatase (from *E. coli*) all from Sigma, St.Louis, MO, USA; *p*-aminobenzoic acid octyl ester (ABOE) labeling kit from Seikagaku Corp., Tokyo, Japan; 1, 2-diamino-4, 5-methylenedioxybenzene dihydrochloride (DMB) from Donjindo Lab., Kumamoto, Japan. GM1 ganglioside was purified from bovine brain in our own laboratory. All other chemicals and reagents were of analytical grade or higher.

Purification of LS and LF

Schematic outline of isolation of crude LPS fractions

The optimized protocol to isolate LOS is shown in Fig. 1. *C. jejuni*, ATCC-43446 (serotype HS19), was grown in *Brucella* Broth with gentle shaking (100–150 rpm) under microaerophilic conditions. The cells were recovered by centrifugation at 4,000 rpm for 30 min and washed twice with saline. The cell pellets were kept frozen at −20° until use. The LOS fraction was extracted from the cell pellets by the hot phenol-water procedure of Westphal [13]. An aqueous phase and a phenolic phase were obtained. The aqueous phase was dialyzed against water. The dialysate was treated with 2 volumes of methanol and 1 volume of chloroform. After the chloroform layer was recovered by partitioning, the aqueous layer was again partitioned with 1 volume of chloroform and 1 volume of water. The chloroform layer was recovered and combined with the initial chloroform layer. Most of the LOS was recovered in the combined chloroform fraction. An additional minor amount of LOS was precipitated from the remaining phenolic phase by adding 9 volume of acetone. Both LOS fractions were combined, dried, and then subjected to alkaline hydrolysis with 25% ammonia at 56° for 48 h. The solution was then dialyzed against water and the retentate was lyophilized.

Separation of LS and LF by using silica gel column chromatography

The LOS fraction, 0.5 g, obtained as described above, was further fractionated by stepwise elution from a silica gel column (13×1.5 cm i.d., Iatrobeads, 6RS-8060, Iatron Laboratories, Inc., Tokyo, Japan) using the following solvents: (1) 60 ml of *n*-propanol; (2) 40 ml of *n*-propanol:H_2O (75:20, v/v); (3) 100 ml of *n*-propanol:H_2O:triethylamine (75:20:5, v/v/v); and (4) 100 ml of *n*-propanol:H_2O:triethylamine (60:20:20, v/v/v). The fractions eluted with solvents 1 and 3 were collected; an aliquot of each was tested by TLC-overlay, and the bulk of each of these samples was evaporated to dryness. For TLC-

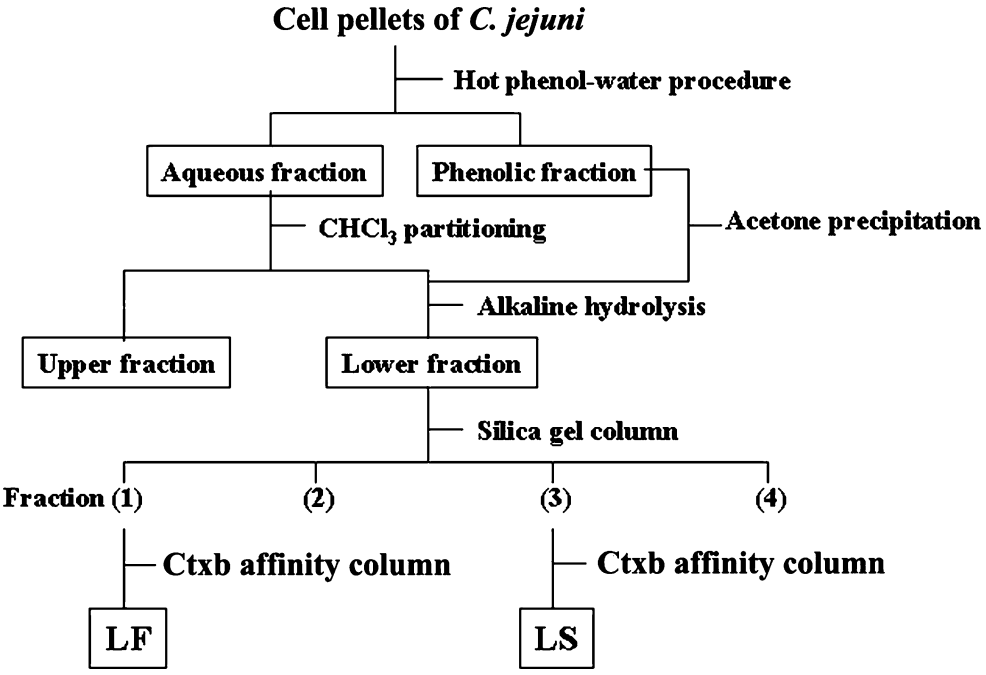

Fig. 1 Isolation scheme for fractions LS and LF from crude LOS fraction. The steps involved in the isolation and purification of LS and LF are shown. For details of each step, see "Materials and methods." The abbreviations used are the following: Ctxb, cholera toxin B subunit; LS, a major of LOS component characterized as a slow-migrating band based on the TLC of Ctxb-overlay; LF, a minor of LOS component characterized as a fast-migrating band on the TLC of Ctxb-overlay. Fractions (1) to (4): stepwise eluting from silica gel column with the following solvents: (1) *n*-propanol; (2) *n*-propanol:H_2O (75:20 v/v); (3) *n*-propanol:H_2O:triethylamine (75:20:5 v/v/v); (4) *n*-propanol:H_2O:triethylamine (60:20:20 v/v/v)

overlay, the sample was first developed using the solvent system of *n*-propanol:H_2O:25% NH_3 (6:3:1, v/v/v). After drying, the plate was overlaid with a Ctxb solution (1:1,000 dilution) as described previously [14].

Affinity chromatography of LS and LF

One mg of Ctxb protein, dissolved in a coupling buffer (0.1 M $NaHCO_3$, pH 8.0), was coupled with 3.5 ml of an affinity gel, CNBr-Sepharose 4B (Sigma, St.Louis, MO, USA) by the procedure previously described [15]. The LOS fractions (10 mg), eluted with solvents 1 and 3, were applied onto an affinity column (column volume, 1 ml) and subjected to stepwise elution with the following solvents: (1) 10 ml of 50 mM PBS; (2) 5 ml of 100 mM $NiCl_2$/ 50 mM PBS buffer; and (3) 5 ml of 1 M PBS buffer. The bound LPS fraction, eluted with solvent 2, was dialyzed against water and lyophilized. The LPS lyophilizate was stored at −20° before use.

TLC-overlay with Ctxb

A portion of the purified LOS fractions, containing LS or LF, was examined by the TLC-overlay method with Ctxb as follows [14]. The LOS fraction and authentic GM1 were applied onto a TLC plate (HPTLC, aluminum-backed silica gel 60 sheet). The plate was developed with the solvent system of *n*-propanol:H_2O:25% NH_3 (6:3:1, v/v/v). After drying, the plate was soaked with 0.1% polyisobutylmethacrylate in *n*-hexane for 1 min. The plate was overlaid with 1% ovalbumin in PBS solution for 20 min and then with the diluted Ctxb solution [horseradish peroxidase (HRP)-conjugated Ctxb, 1:1,000, or 5,000 dilution by 1% ovalbumin/PBS solution]. The original Ctxb solution was 1 mg /ml in PBS solution, and the labeling ratio was 2.38 mg of horseradish peroxidase per mg of Ctxb (1:1,000 or 1:5,000 dilution) in PBS solution containing 1% ovalbumin and 0.05% Tween 20. The plate was overlaid for 16 h at room temperature. The plate was washed with 1% ovalbumin in PBS solution containing 0.05% Tween 20. After washing, the plate was overlaid with OPD peroxidase substrate. The plate was washed with distilled water and dried under air. Bands were recorded by an imaging scanner.

Structural analysis of LS

Schematic outline of LS analysis

The schematic outline of LS analysis is shown in Fig. 2. Briefly, the oligosaccharide was released by mild acid hydrolysis and separated by ultracentrifugation and Bio-Gel P-2 gel filtration. The oligosaccharide was labeled by reductive amination with ABOE [16] or by quinoxalinone formation with DMB [17]. To determine carbohydrate structural linkages, the ABOE-oligosaccharide and the DMB-oligosaccharide were isolated by Bio-Gel P-2 gel filtration. Finally, the molecular mass and carbohydrate linkage were determined by MALDI-TOF mass spectrometry.

To determine the carbohydrate composition, the ABOE- or DMB-oligosaccharide was subjected to acid hydrolysis with 2 N HCl /2 M trifluoroacetic acid or 25 mM sulfuric acid, respectively, and decomposed into neutral monosaccharides or α-keto acid monosaccharides; the resulting monosaccharides labeled by ABEE or DMB were analyzed by HPLC [16–18].

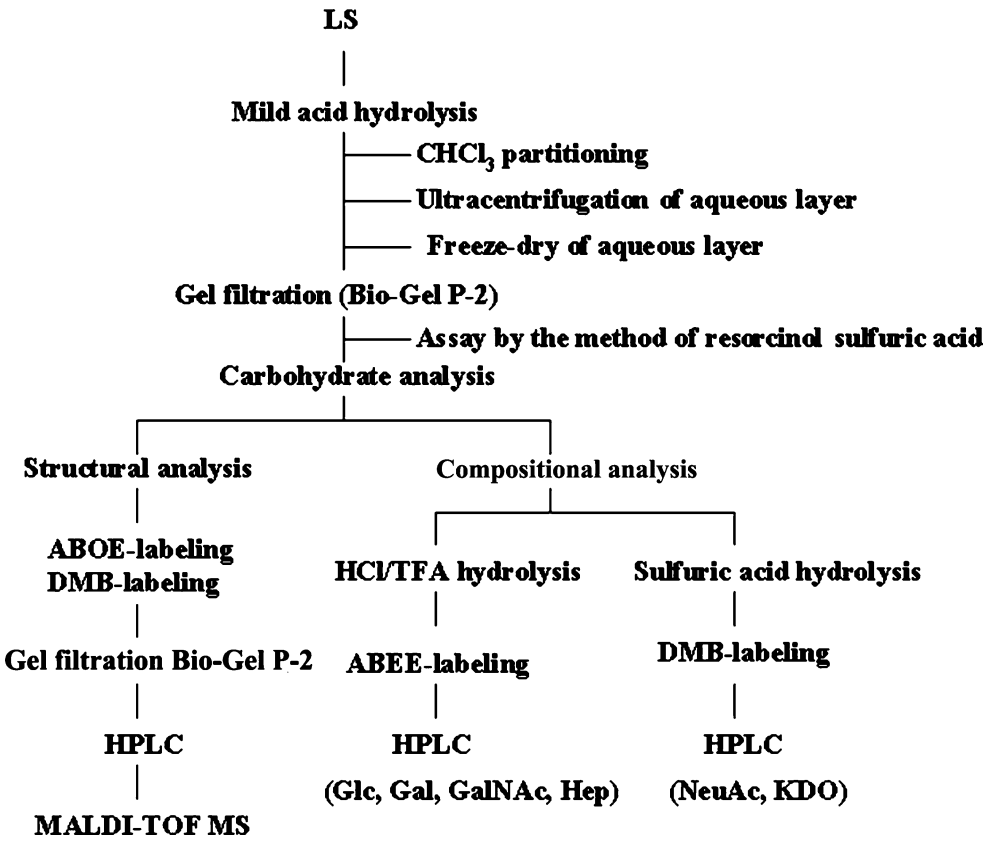

Fig. 2 Scheme for structural analysis of LS. The steps involved in the analysis flow chart are shown. For details of each step see "Materials and methods." Structural analysis involved carbohydrate linkage determination of the oligosaccharides obtained after mild acid hydrolysis of LS. The molar ratios of monosaccharides were obtained after hydrolysis of LS in 2 N HCl and 2 M trifluoroacetic acid/water or 25 mM sulfuric acid

Oligosaccharide isolation

The affinity-purified LOS (10 mg) was subjected to mild acid hydrolysis with 10 ml of 1% acetic acid in water for 1 h at 90°C. After being neutralized with 1 M NaOH, the reaction mixture was ultracentrifuged (Beckman Optima XL-100K Ultracentrifuge, rotor SW55Ti; 100,000×g, 4°C, 1 h). The supernatant was recovered and then washed with an equivalent volume of chloroform. After partitioning, an aqueous solution was recovered and freeze-dried. The residue was dissolved in a small volume of water, applied to a Bio-Gel P-2 column (45×1 cm i.d., BioRad, Hercules, CA, USA), and eluted with 0.1 M pyridine-acetic acid buffer (pH 5.3)[16]. One ml-fractions were collected with a fraction collector. The sugar content in each fraction was determined by the resorcinol-sulfuric acid method using mannose as a standard [19]. The resorcinol-sulfuric acid positive fractions containing oligosaccharides were pooled and dried *in vacuo*.

Carbohydrate compositional analysis

Glucose (Glc), galactose (Gal), L-*glycero*-D-*manno*-heptose (Hep), and *N*-acetylgalactosamine (GalNAc) were analyzed by the method of Fuji *et al.* [18, 20]. Briefly, the purified oligosaccharide fraction was hydrolyzed in 2 N HCl and 2 M trifluoroacetic acid for 4 h at 100°C, dried down, and converted to *p*-aminobenzoic acid ethyl ester (ABEE)-labeled monosaccharides. The monosaccharides (Glc, Gal, or Hep) were then analyzed by high-performance liquid chromatography (HPLC, Model LC-VP, equipped with a Model RF 10AXL fluorescence detector, Shimadzu, Kyoto, Japan) on a Honen Pak C18 column with a linear gradient elution from 0.02 to 0.2 M potassium borate buffer / CH_3CN (94:6, v/v) at a flow rate of 1.0 ml/min for 50 min. GalNAc was analyzed as the ABEE-labeled galactosamine by HPLC with an isocratic elution of 0.02% trifluroroacetic acid/CH_3CN (90:10, v/v) at a 1.0 ml/min of flow rate for 50 min. Elution was monitored by a fluorescence detector at an excitation wavelength of 305 nm and an emission wavelength of 360 nm.

DMB-labeled α-keto acid monosaccharides, such as *N*-acetylneuraminic acid (NeuAc), *N*-glycolylneuraminic acid (NeuGc), and 2-keto-3-deoxyoctanoic acid (Kdo), were analyzed by HPLC using an ODS column by Axxiom chromatography equipped with a fluorescence detector at an excitation wavelength of 373 nm and an emission wavelength of 448 nm. The molar ratio of DMB-NeuAc and ABEE-Gal was calibrated from estimating the correction factor between fluorescence intensities using labeled monosaccharides from sialyllactose.

Oligosaccharide analysis

The oligosaccharide fraction was derivatized using an ABOE-labeling kit, and the derivatives were separated on

a Bio-Gel P-2 column (45×1 cm i.d., BioRad, Hercules, CA, USA) by elution with 0.1 M pyridine-acetic acid buffer (pH 5.3). Fractions of 1 ml each were collected. The fluorescence intensity in each fraction was measured using a fluorescence spectrophotometer (Model F-2500, Hitachi, Tokyo, Japan). Fractions containing ABOE-labeled oligosaccharides were collected, pooled, and evaporated to dryness in vacuo. The dried residue was dissolved in water and analyzed by HPLC on a Honen Pak C18 column (Seikagaku Corp. Tokyo, Japan), programmed with a linear gradient elution from 10% of 0.1 M aqueous ammonium acetate (pH 4.0):CH_3CN [55:45 (v/v) in 75:25 (v/v)] to 80% of 0.1 M aqueous ammonium acetate (pH 4.0):CH_3CN [55:45 (v/v) in 75:25 (v/v)] for 40 min. Elution was monitored by a fluorescence detector at an excitation wavelength of 314 nm and an emission wavelength of 368 nm [21]. The fluorescent peak at the retention time of 21.5 min, corresponding to that of the ABOE-labeled oligosaccharide, was recovered from HPLC and desalted by a Sep-Pak C18 cartridge.

The oligosaccharide fraction was derivatized using the DMB-labeling method, and the derivatives were separated by a Bio-Gel P-2 column (45×1 cm i.d., BioRad, Hercules, CA, USA) by elution with water. Fractions of 1 ml each were collected, and the fluorescence intensity in each fraction was measured using a fluorescence spectrophotometer (Model F-2500, Hitachi, Tokyo, Japan). Fractions containing DMB-labeled oligosaccharides were collected, pooled, and evaporated to dryness *in vacuo*. The DMB-labeled oligosaccharides were analyzed by HPLC using an ODS-column Axxiom chromatography with a fluorescence detector at an excitation wavelength of 373 nm and an emission wavelength of 448 nm. The fluorescent peak at the retention time of 26.1 min, corresponding to that of the DMB-labeled oligosaccharide, was recovered from HPLC and desalted by a Sep-Pak C18 cartridge.

The ABOE-labeled oligosaccharides and the DMB-labeled oligosaccharides obtained from the Sep-Pak C18 cartridge were analyzed by Matrix-Assisted Laser Desorption Ionization-Time of Flight (MALDI-TOF) mass spectrometry using a Model 4700 Proteomics Analyzer (Applied Biosystems, Foster City, CA, USA) equipped with a nitrogen UV laser (λ=337 nm) with a matrix of 2,5-dihydroxybenzoic acid at a concentration of 10 mg/ml in 10% aqueous ethanol.

Structural determination of LF

Schematic outline of LF analysis

The schematic outline of LF analysis is shown in Fig. 3. The molecular weight of the purified LF was determined by MALDI-TOF mass spectrometry. Phosphate was released from the purified LF by alkaline phosphatase treatment as described in the method of Gray *et al.* [22]. After chloroform partitioning, the phosphate content of the aqueous layer was quantitated by the method of Touster *et al.* [23]. The phosphate content of the chloroform layer was quantitated by the method of Bartlett *et al.* [24]. The chloroform layer was then dried down by evaporation and subjected to hydrazinolysis and *N*-acetylation. After hexane partitioning, the aqueous layer was evaporated to dryness, and the sample was passed through a Dowex 50WX-8 column. The effluent was concentrated, and the *N*-acetylglucosamine content was determined by a modified method of Morgan-Elson [25]. The hexane layer was dried down, and the free fatty acids were analyzed by the method of Duncombe and Rising [26].

Chemical analysis and quantitation of components of LF

Alkaline phosphatase treatment The purified LF (20 mg) was treated with alkaline phosphatase (from *E. coli*, Sigma, St. Louis, MO, USA) using the method of Gray *et al.* [22]. Briefly, 1 ml of alkaline phosphatase solution containing 50 units of the enzyme in 0.05M $(NH_4)_2CO_3$, pH 9.6, was incubated with the purified LF (20 mg), covered with 0.1 ml of toluene to retard bacterial growth, and incubated for 48 h at 37°. After incubation, 4 ml of chloroform was added, and the solution was separated to upper and lower phases. The aqueous layer was washed twice with 4 ml of chloroform. The combined chloroform layers and the aqueous layers were used for hydrazinolysis and phosphate determination, respectively.

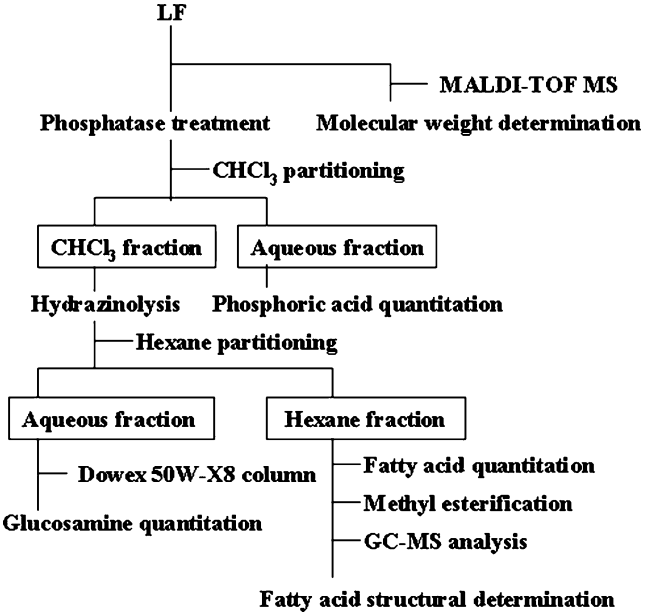

Fig. 3 Scheme for structural analysis of LF. The steps involved in the analysis flow chart are shown. For details of each step see "Materials and methods"

Hydrazinolysis and N-acetylation After alkaline phosphatase treatment, the phosphate-free LF recovered from the chloroform layer was subjected to hydrazinolysis. Briefly, 10 mg of the phosphoric acid-free LF was heated with 0.5 ml of hydrazine for 12 h at 100°C. The reaction solution was dried by evaporator and then partitioned by 2 ml of hexane and 1 ml of water. After the partitioning, the aqueous layer was dried by evaporation, dissolved with 1 ml of saturated $NaHCO_3$ in water and 0.1 ml of acetic anhydride, and then mixed for 30 min on ice. After N-acetylation, the reaction mixture was passed through a Dowex 50W-X8 column (column volume 1 ml), followed by elution with 5 ml of water. An aliquot of the effluent was dried by evaporation, and the *N*-acetylglucosamine content was determined by the modified method of Morgan-Elson [25].

Quantitation of phosphate The released phosphate obtained from the aqueous layer by alkaline phosphatase treatment was measured by the method of Aronson and Touster [23]. Briefly, 2 ml of the upper layer solution was mixed with 0.5 ml of 2.5% ammonium molybdate in 2.5 M sulfuric acid and 0.2 ml of a reducing reagent that contained 10 mg of 1-amino-2-naphthol-4-sulfonic acid, 60 mg of sodium bisulfite, 60 mg of sodium sulfite, and 5.4 ml of water. The mixed samples were let stand for 20 min at room temperature. The OD at 660 nm was measured by a spectrophotometer using inorganic phosphate salt as the standard. Any bound phosphate in LF after the alkaline phosphatase treatment was measured by the method of Bartlett [24]. Briefly, 0.5 ml of the chloroform layer solution was dried down by a stream of nitrogen, mixed with 0.125 ml of 10 N H_2SO_4, and heated for 3 h at 150°C, followed by the addition of 10 μl of 30% H_2O_2 and heating for 2 h at 150°C. After cooling on ice, an aliquot of the sample was mixed with 1.15 ml of 0.22% ammonium molybdate, followed by the addition of 0.05 ml of Fiske-Subbarow reagent containing 15% sodium bisulfite, 0.25% 1-amino-2-napthol-4-sulfonic acid, and 0.5% sodium sulfite in water. Subsequently, the sample solution was mixed and heated for 7 min at 100°C, followed by cooling on ice. The OD at 830 nm in the aliquot was measured by a spectrophotometer using inorganic phosphoric acid as the standard.

Quantitation of neutral monosaccharides Neutral monosaccharides were measured by the resorcinol-sulfuric acid method [19]. A 100-ng sample of LF was mixed with 0.1 ml of 0.01 M sodium acetate and 0.1 ml of resorcinol (6 mg/ml), and then followed by the addition of 0.5 ml of 75% (v/v) sulfuric acid/water 0.5 ml. The mixture was heated on a block heater for 30 min at 90°C. The solution was cooled on an ice bath and kept in the dark. The OD at 430 nm was measured by a spectrophotometer using mannose as the standard.

Quantitation of N-acetylglucosamine *N*-Acetylglucosamine was determined by the modified method of Morgan-Elson [25]. After hydrazinolysis and *N*-acetylation, the sample was dissolved in 0.5 ml of water and mixed with 0.1 ml of 1.6 M boric acid/water (adjusted to pH 9.1 by 1 M KOH); the sample was heated for 3 min at 100°C and then cooled on ice. The reaction solution was mixed with 3.0 ml of DMAB reagent (0.6 M *p*-dimethylaminobenzaldehyde/12.5% of 10 N HCl in acetic acid), heated for 20 min at 37°C, cooled on ice, and centrifuged at 2,500 rpm for 5 min. The OD at 530 nm in aliquot was measured by a spectrophotometer using *N*-acetylglucosamine as the standard.

Quantitation of fatty acids After hydrazinolysis, the hexane layer was dried in an evaporator. The total fatty acid level was quantitated by the method of Duncombe *et al.* [26]. Briefly, the dried sample was dissolved in 3 ml of chloroform, mixed with 1.5 ml of cupric reagent (1 M triethanolamine:1 M acetic acid:6.45% cupric nitrate, 9:1:10, by volume), and followed by shaking for 2 min at room temperature and centrifuging for 5 min. A chloroform phase (1.8 ml) was separated and mixed with 0.5 ml of 0.1% sodium diethyldithiocarbamate/2-butanol (w/v). The OD at 440 nm in an aliquot was measured using stearic acid as the standard.

GC-MS analysis of fatty acids After evaporation of the hexane layer, the fatty acids were subjected to esterification with 1 N HCl in methanol for 16 h at 80°C. The aqueous layer was partitioned three times with *n*-hexane. The hexane layers were pooled and evaporated under nitrogen, and the residues were examined by TLC-iodine staining after development in the solvent system of *n*-hexane: diethylether (8:2, v/v). TLC-iodine staining revealed that LF contained an equal amount of 2-and 3-hydroxy fatty acids. Each band of the fatty acid methyl esters was separated by preparative TLC. After preparative TLC, each of the fatty acid methyl esters was analyzed by gas chromatography-mass spectrometry (GC-MS) with a Hewlett-Packard GC-MS (5972 MS and 5890 GC) Chemical Station equipped with a special-performance capillary column DB-1 (50 m× 0.25 mm) coated with dimethylpolysiloxane (film 0.25 μm). Analysis was performed under the following gradient conditions: initial temperature, 100°C; rate, 10°C/min; final temperature, 220°C.

Ctxb binding and ligand-precipitation of LS and LF using sucrose density gradient separation

Samples of 100 μg each of LS, LF, LA1, LA2, LF/p, LA1/p, LA2/p, or GM1 were incubated with biotin-labeled Ctxb (10 μg) in PBS (500 μl) for 30 min at room temperature before transfer to the top of a linear gradient of 8–30%

sucrose in 4.3 ml of PBS solution and ultracentrifugation using a Beckman Coulter XL-100K Optima Ultracentrifuge (Beckman rotor 55Ti, 200,000×g, 4°C, 16 h). Eight 600-μl fractions were collected from the top [12]. Each sample was then subjected to SDS-PAGE in 14% gel (non-reducing conditions) according to the method of Laemmli [27]. After electrophoresis, the proteins were transferred to a nitrocellulose membrane (Trans-Blot Transfer medium, 0.45 μm, BioRad, Hercules, CA, USA) in a transfer buffer containing Tris buffer (BioRad, Hercules, CA, USA) and 20% methanol in water. Non-specific binding sites were blocked with 5% milk casein in PBS containing 0.1% Tween 20 for 1 h. The blots were washed three times for 10 min each in PBS containing 0.1% Tween 20, then incubated for 30 min at room temperature with horseradish peroxidase-conjugated avidin (1:500 diluted by PBS, BioRad, Hercules, CA, USA). After removal of the unbound HRP-avidin by rinsing 3× 10 min in PBS containing 0.1% Tween 20, the blots were visualized on an X-ray film by the addition of ECL Western blotting detection reagent (Amersham Pharamacia Biotech).

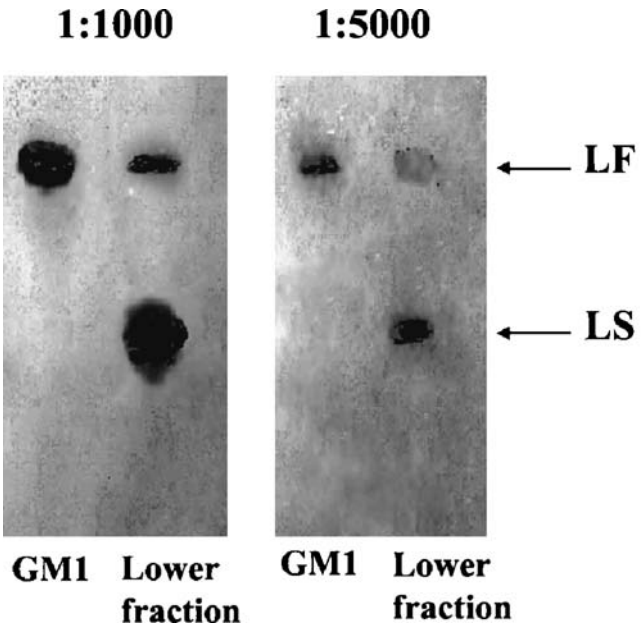

Fig. 4 TLC-overlay of LS and LF. Samples of 100 ng of the lower fraction (see Fig. 1) before Ctxb-affinity column chromatography were developed on the TLC plate using *n*-propanol:H_2O:25% NH_3 (6:3:1, v/v/v) as the developing solvent and the plate was then examined by TLC-overlay at 1:1,000 (1 μg/ml) and 1:5,000 (0.2 μg/ml) dilution of Ctxb in PBS buffer containing 1% ovalbumin and 0.05% Tween 20

Results

TLC-overlay of LS and LF with Ctxb

The lower fraction was examined by a TLC-overlay method with Ctxb after the plate was developed using n-propanol: H_2O:25% NH_3 (6:3:1, v/v/v) as shown in Fig. 4. TLC-Ctxb overlay revealed a slow-migrating (LS) band and a fast-migrating (LF) band. LF stained weakly with a Ctxb solution at 1:5,000 dilution and needed a higher concentration (1:1,000 dilution) of Ctxb than LS for clear staining.

Extraction of LOS and purification of LS and LF

The LOS fraction (500 mg) was applied to a silica gel column, followed by a stepwise elution. LF and LS were separated and eluted in fractions 1 or 3 as shown in Fig. 5a. The yield of fractions 1 and 3 was about 8 mg and 32 mg, respectively. To isolate Ctxb-binding components of fractions 1 and 3, each fraction was applied to an affinity column immobilized with Ctxb, and the bound component was eluted into fraction 2 (Fig. 5a*A* and *B*). LF and LS each gave a single band by TLC-overlay, and the yield was 0.5 mg and 3 mg, respectively (Fig. 5c).

Structural analysis of LS

Monosaccharide compositional analysis

The purified LS was chemically analyzed by the method according to each step of the schematic outline as shown in Fig. 2. After acetic acid hydrolysis, the oligosaccharides in the lyophilizate were separated by a Bio-Gel P-2 column (Fig. 6a). Fractions 16 to 30 were collected, pooled, and freeze-dried. Subsequently, the oligosaccharides were subjected to carbohydrate compositional analysis by ABEE-labeling and DMB-labeling. Figure 6b shows the HPLC profiles of the monosaccharide carbohydrate composition of LS. Table 1 shows the monosaccharide composition of the oligosaccharide of the Ctxb-binding fraction as having the molar ratio: Gal:GalNAc:Glc:Hep, 2.13:0.95:1.0:1.89 as shown in Fig. 6b*A* and Table 1; $GalNH_2$:Glc/Gal/Hep in Fig. 6b*B*. Analysis of the DMB-labeled α-keto acid monosaccharides revealed the molar ratio of NeuAc:Kdo, 1.0:1.28, as shown in Fig. 6b*C* and Table 1.

Analysis of ABOE-or DMB-labeled oligosaccharides

After separation of the oligosaccharides by Bio-Gel P-2 column chromatography, the pooled fractions of oligosaccharides were derivatized using ABOE or a DMB labeling kit, and the derivatives were separated on a Bio-Gel P-2 column. The fluorescence intensity in each fraction was measured using a fluorescence spectrophotometer. Fractions containing ABOE-or DMB-labeled oligosaccharides (fractions 22–36 for ABOE-oligosaccharides and fractions 11–24 for DMB-labeled oligosaccharides) were collected, pooled, and evaporated to dryness in vacuo (Fig. 6c,e).

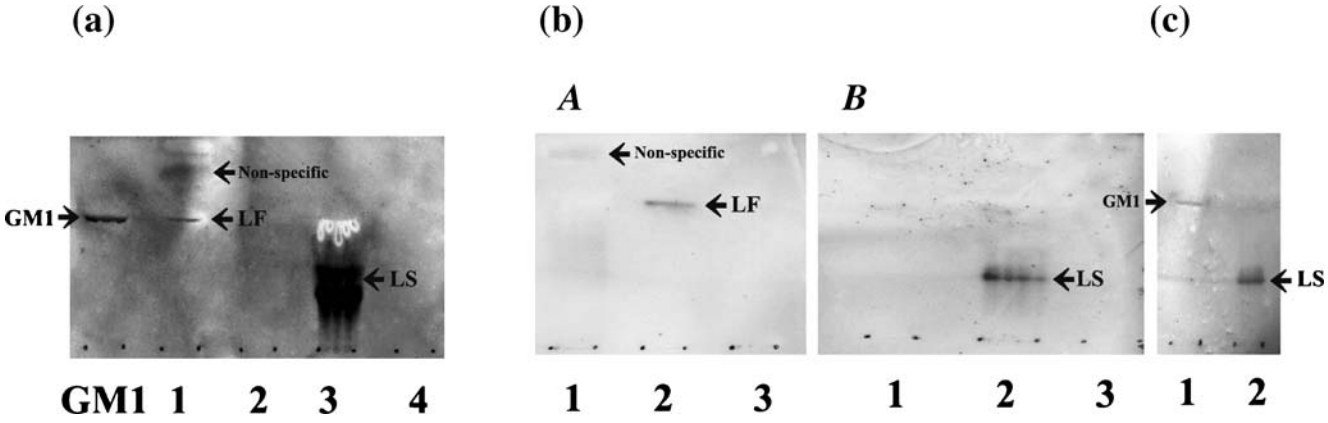

Fig. 5 Purification of LS and LF by silica gel column chromatography (**a**) and Ctxb-affinity chromatography (**b**). LS and LF were detected by TLC-overlay at 1:1,000 dilution of Ctxb solution. **a**: TLC-overlay at 1:1,000 dilution of Ctxb solution after silica gel column chromatography. GM1, authentic GM1; lane 1, fraction eluted by *n*-propanol; lane 2, fraction eluted by *n*-propanol:water (75:20 v/v); lane 3, fraction eluted by *n*-propanol:water:triethylamine (75:20:5 v/v/v); lane 4, fraction eluted by *n*-propanol:water:triethylamine (75:20:20 v/v/v). **b**: TLC-overlay at 1:1,000 dilution of Ctxb solution after Ctxb-affinity column chromatography (*A*, *B*) of fraction 1 or 3 obtained from silica gel column chromatography. Lane 1, fraction eluted by 50 mM PBS buffer; lane 2, fraction eluted by 100 mM $NiCl_2$/50 mM PBS buffer; lane 3, fraction eluted by 1 M PBS buffer. **c**: lane 1, purified GM1 from affinity chromatography; lane 2, purified LS from affinity chromatography

The dried residue of ABOE-labeled oligosaccharide solution was dissolved in water and analyzed by HPLC. Fluorescent peak A was recovered from HPLC and used for mass spectrometric analysis (Fig. 6d). The dried residue of DMB-labeled oligosaccharide solution was dissolved in water and analyzed by HPLC under the same conditions as described previously [17]. Fluorescent peak B was recovered from HPLC and used for mass spectrometric analysis (Fig. 6f).

Peak A shown in Fig. 6d and peak B in Fig. 6f were analyzed by MALDI-TOF mass spectrometry, and the results are shown in Fig. 7a,b, respectively. The fraction corresponding to peak A revealed a distinct mass signal at m/z 1262.1 that was assigned as the protonated molecular ion [M+H]. The most prominent signals at m/z 1284.6 and m/z 1307.1 corresponded to [M+Na] and [M+2Na], respectively. The signal at m/z 993.1 was in agreement with the fragment ion [M+Na−NeuAc]. For the fraction corresponding to peak B, a mass signal at m/z 832.2 was assigned as the protonated molecular ion [M+H]. The signals at m/z 876.5, m/z 854.2, and 692.1 were in agreement with [M+2Na], [M+Na], and [M+Na−Glc], respectively. As shown in Table 1, the ratio of monosaccharides of ABOE-oligosaccharides and DMB-oligosaccharides could be deduced to be consistent with the following: structure I, Gal:GalNAc:Hep:NeuAc in the molar ratio of 2:1:1:1; and structure II, Glc:Hep:Kdo in the molar ratio of 1:1:1.

From the mass spectra of peaks A and B and their monosaccharide compositional ratios, LS was deduced to be an octasaccharide containing a phosphate residue: Gal-GalNAc-(NeuAc)Gal-Hep-(Glc;PO_3H)Hep-Kdo as shown in Fig. 8a. A full-length oligosaccharide could not be recovered, probably due to decomposition between the disaccharide linkage of Hep of the octasaccharide during acetic acid hydrolysis.

Structural analysis of LF

Compositional analysis

The purified LF was analyzed by MALDI-TOF mass spectrometry. The signals at m/z 1882.1, m/z 1859.1, and m/z 1837.1 are in agreement with [M+2Na], [M+Na], and [M+H], respectively. The most prominent signal at m/z 667.1 is assigned as [RCOOH] (Fig. 7c).

The purified LF (20 mg) was treated with alkaline phosphatase by the method of Gray *et al.* [22]. After alkaline phosphatase treatment, the remnant of LF was tested by TLC using Dittmer staining and TLC-Ctxb overlay. Dittmer staining showed LF as a single band on TLC, but that band disappeared after alkaline phosphatase treatment (Fig. 9a). Deprivation of the phosphate group caused the disappearance of the Ctxb-binding activity of LF as shown in Ctxb-overlay (Fig. 9b). Lipid A binding activity to Ctxb was demonstrated by authentic lipid A with mono-or bisphosphorylation (LA1 or LA2), derived from the LPS of *E. coli* (Fig. 9b).

Subsequent to chloroform partitioning, free and bound phosphates were determined by the method as described in "Material and methods" (Fig. 3). About 96% of the total phosphate was released as inorganic phosphate. The total phosphate amount was estimated as 1.90 mg (19.39 μmol) per 20 mg of LF. The chloroform layer was dried by evaporation, and the residue was subjected to hydrazinolysis. After hexane partitioning, the aqueous layer was dried by evaporation, and the residue was subjected to

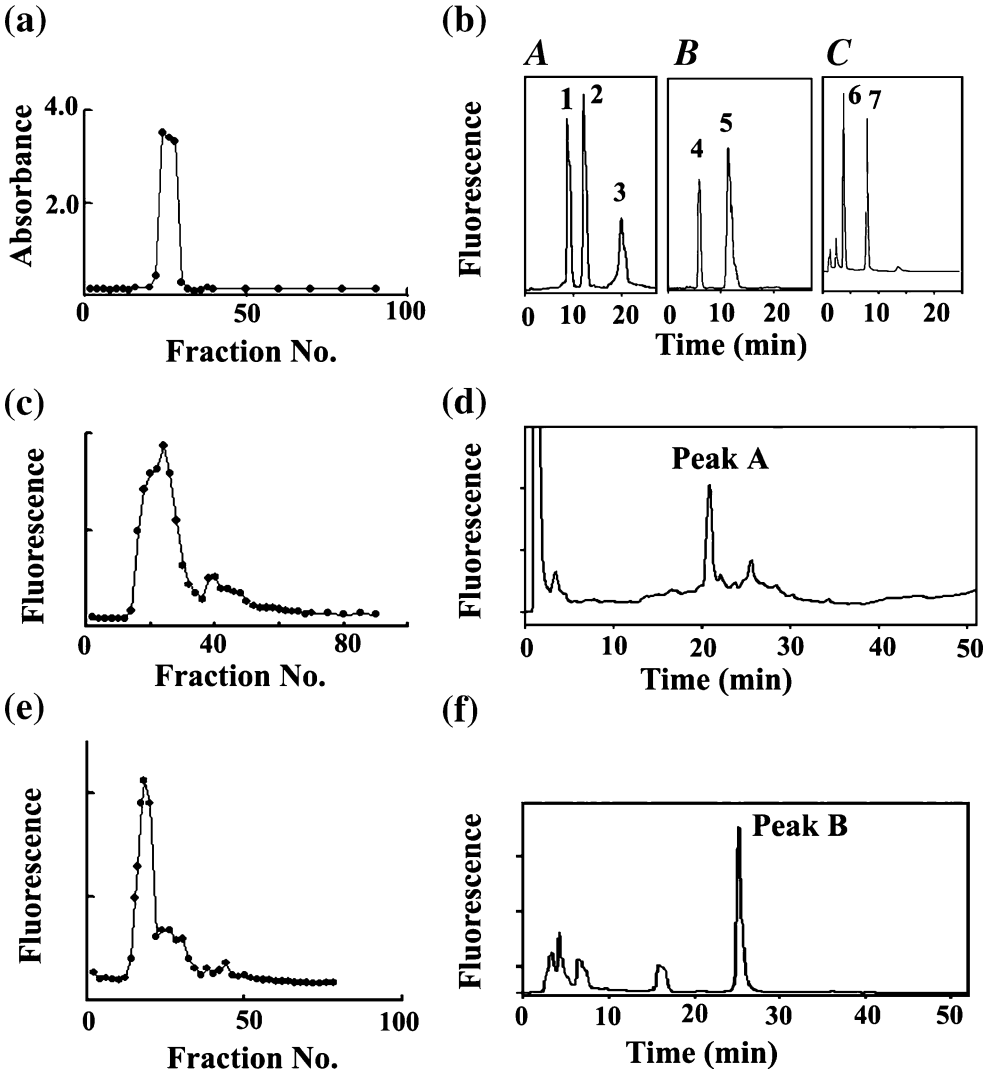

Fig. 6 Structural analysis of LS. **a**: The elution profile of the oligosaccharides obtained from mild acid hydrolysis of LS with 1% acetic acid/water for 1 h at 90°C on Bio-Gel P-2 column chromatography (see Fig. 2). Detection of oligosaccharides was achieved by the resorcinol-sulfuric acid method (see in "Materials and methods"). **b**: HPLC separation of ABEE-labeled monosaccharides (*A*, *B*) on Honen Pak C18 column or DMB-labeled α-keto acid monosaccharides (*C*) on ODS column . Peak 1, Hep; 2, Gal; 3, Glc; 4, $GalNH_2$; 5, Glc/Gal/Hep; 6, Kdo; 7, NeuAc. **c**: The elution profile of the ABOE-labeled oligosaccharides on Bio-Gel P-2 column chromatography (see Fig. 2). Detection was achieved by a fluorescence spectrophotometer at an excitation wavelength of 314 nm and an emission wavelength of 368 nm. **d**: HPLC separation of the ABOE-labeled oligosaccharides on Honen Pak C18 column at an excitation wavelength of 314 nm and an emission wavelength of 368 nm. **e**: The elution profile of the DMB-labeled oligosaccharides on Bio-Gel P-2 column chromatography (see also Fig. 2). Detection was achieved by a fluorescence spectrophotometer at an excitation wavelength of 373 nm and an emission wavelength of 448 nm. **f**: HPLC separation of the DMB-labeled oligosaccharides on ODS column at an excitation wavelength of 373 nm and an emission wavelength of 448 nm

Dowex 50W-X8 column chromatography. An effluent was dried by evaporation. The amount of *N*-acetylglucosamine was determined by a modified method of Morgan-Elson [25] and converted into that of glucosamine disaccharide. The amount of glucosamine disaccharide was estimated to be 3.51 mg (9.44 μmol) per 20 mg of LF.

The amount of fatty acids was determined by the method of Duncombe and Rising [26] and converted into a molar amount using a molecular weight corresponding to m/z 667.1 as assigned by MALDI-TOF mass spectrometry. The concentration was estimated to be 14.01 mg (21.00 μmol) per 20 mg of LF.

No involvement of neutral monosaccharides (Glc or Gal) or α-keto acid monosaccharides (Kdo or NeuAc) was confirmed by the resorcinol-sulfuric acid reagent or HPLC analysis, respectively, as described in Materials and Methods. Ethanolamine was not identified in LF by the method of Nojima *et al.* [28].

Compositional analysis of LF is presented in Table 2. The molar ratio of phosphoric acid: glucosamine disaccha-

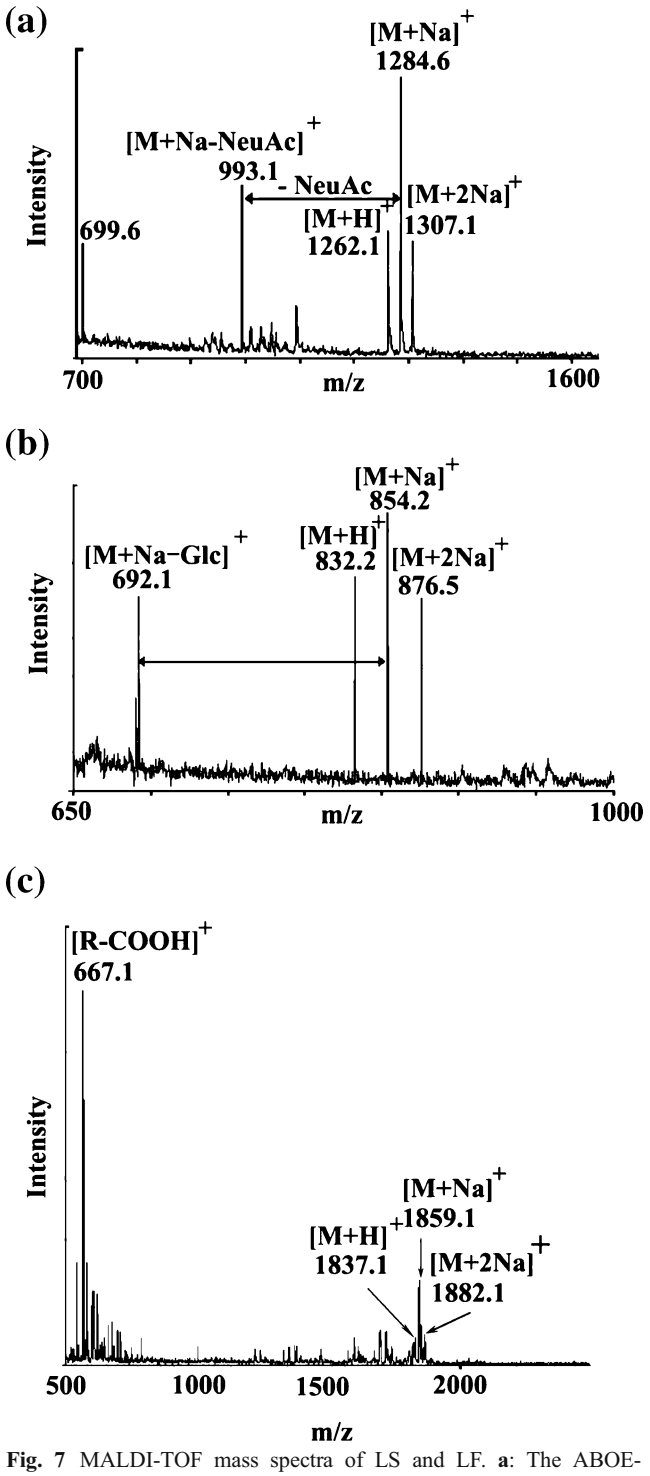

Fig. 7 MALDI-TOF mass spectra of LS and LF. **a**: The ABOE-labeled oligosaccharides (see peak A in Fig. 6d) obtained from mild acid hydrolysis of LS. **b**: The DMB-labeled oligosaccharides (see peak B in Fig. 6f) obtained from mild acid hydrolysis of LS. **c**: LF

ride:fatty acid was 1.88:1.0:2.22, suggesting that most of the glucosamine residues were phosphorylated and that fatty acid was attached to the 2-and 2′-positions of the glucosamine disaccharide. Based on the molar ratio, LF was characterized as lipid A (Fig. 8b).

GC-MS analysis of fatty acids

The fatty acids of LF were converted to their methyl esters and tested by TLC-iodine staining, which revealed the presence of two approximately equal bands, corresponding to authentic methyl esters of 2-hydroxy tetracosanoic acid and 3-hydroxy octadecanoic acid (see also below) (Fig. 9c). Each of the TLC bands was separated by preparative TLC. GC analysis of the upper and lower constituents resulted in a single peak in each case corresponding to 2-hydroxytetracosanoic acid and 3-hydroxy octadecanoic acid by comparing their retention times, 49.12 min and 22.27 min, respectively. Mass spectrometric analysis of the former GC peak confirmed 2-hydroxytetracosanoic acid with the signals at m/z 398, m/z 339, and m/z 103, which are in agreement with ions [M], [M-$COOCH_3$], and [CH_2CHOH-$COOCH_3$], respectively. The latter GC peak represents 3-hydroxyoctadecanoic acid with the signals at m/z 314, m/z 73, and m/z 103, which are in agreement with ions [M], [CH_2COOCH_3], and [$CHOHCH_2COOCH_3$], respectively. From the fatty acid fragment ion at m/z 667 in the MALDI-TOF mass spectrum, the fatty acid is presumed to be involved in LF in an ester form of 2-hydroxytetracosanoic acid and 3-hydroxy octadecanoic acid, as shown in Fig. 8c. Based on the above analysis, the proposed structure of LF is shown in Fig. 8b.

Binding profile of LF to Ctxb

We found that two distinct molecules, LS and LF, can bind with high and low affinities, respectively, to Ctxb. To confirm the formation of an LF-Ctxb complex, biotin-labeled Ctxb was incubated with LF, after which the samples were separated by sucrose density gradient centrifugation. Eight 600-μl fractions were collected and examined by SDS-PAGE (Fig. 10). The expression profile

Table 1 Carbohydrate compositional analysis of the oligosaccharide of LS

	Gal	GalNAc	Glc	Hep	NeuAc	Kdo
(method)						
ABEE	2.13[a]	0.95	1.0	1.89		
DMB					1.0	1.28
(assignment)						
Structure I (Peak A)	2	1		1	1	
Structure II (Peak B)			1	1		1

Neutral or α-keto acid monosaccharides were converted into ABEE- or DMB-derivatives, respectively, and analyzed by HPLC with a fluorescence detector. The molar ratio was estimated by fluorescence intensity ratio and was corrected with NeuAc/Gal fluorescence intensity ratio of authentic sialyllactose. [a] molar ratio of carbohydrates.

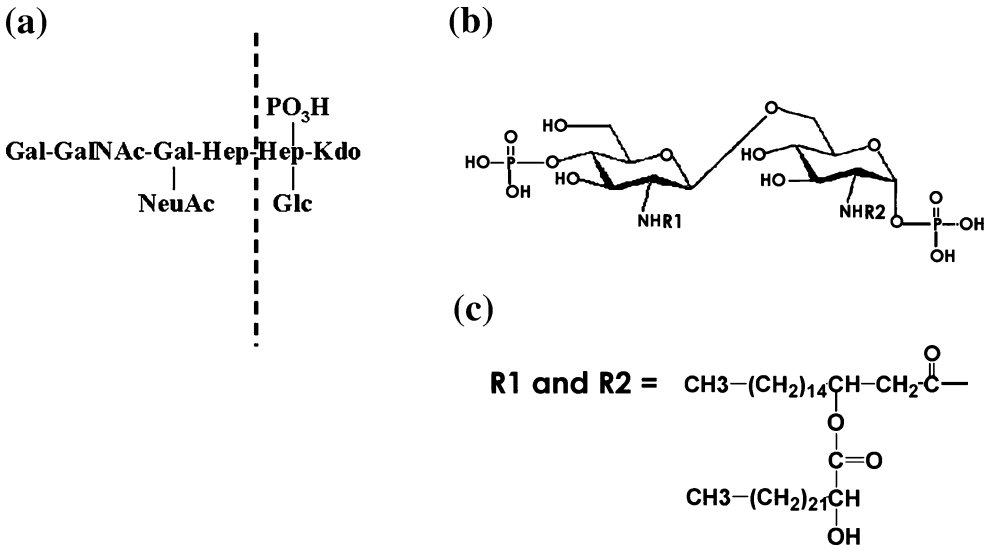

Fig. 8 Proposal structure of LS and LF. **a**: LS is composed of components in peak A and peak B of Fig. 6d and f. A *broken line* indicates division into the pentasaccharide and trisaccharide of components in peaks A and B. **b**: LF is characterized as lipid A with the following structure: 1, 4′-bisphosphoryl glucosamine disaccharide N, N′-acylated by 3-(2-hydroxytetracosanoyloxy) octadecanoic acid at 2- and 2′-positions. **c**: R1 and R2 are acyl groups consisted of 3-(2-hydroxytetracosanoyloxy) octadecanoic acid

of LF was compared with those of GM1 and LS. Dense biotin-labeled Ctxb was found in fractions 4 and 5 after incubation with BSA. GM1-precipitated biotin-labeled Ctxb, however, was found in bottom fractions 8 and 9. A similar result was obtained from precipitation with LS. LF was less effective than either GM1 or LS in forming a complex with Ctxb-biotin, as indicated by the disperse complex distribution of Ctxb in fractions 4, 5, 7, and 8. We hypothesized that LF formed a complex with Ctxb by interacting with the disaccharide with its phosphate moiety, and we determine if complex formation occurred before and after alkaline phosphatase treatment. As shown in Fig. 10c, phosphatase-treated LF (LF/p) lost its binding affinity to Ctxb. Authentic lipid A with either mono- or bisphosphorylation was also tested for complex formation and resulted in weak complex formation as did LF (Fig. 10b,c). LA2, which contains both phosphate groups, possessed stronger affinity toward Ctx-biotin than did LA1, which has only one phosphate group. The capability of complex formation between Ctxb and authentic lipid A (LA1 and LA2) decreased after phosphatase treatment (LA1/p and LA2/p, Fig. 10c). The results suggest that the presence of both phosphate moieties is necessary for optimal interaction with Ctxb.

Discussion

Infectious microbial agents have long been thought to play an important role in the pathogenic mechanisms of a variety of autoimmune diseases. Molecular mimicry is a potential mechanism to account for the cross-reactivity of microbial components, such as peptides or carbohydrates, to certain self-epitopes in tissues to induce autoimmunity [29–31]. However, it has been difficult to prove that a microbial peptide is able to function as a pathogenic antigen because not all amino acid sequences are capable of inducing effective autoimmunity [32]. Molecular mimicry is valid only when a specific peptide with a defined amino acid sequence can represent a specific tissue epitopic structure that is recognized by an autoantibody. Carbohydrate mimicry is under a similar constraint as peptide mimicry. Of course, we should not ignore the possibility that molecular mimicry might be associated with an initial activation of autoreactive *T* cells that are involved in the mechanism of autoimmune diseases [33].

We are interested in the specificity and cross-reactivity of serum antibodies against gangliosides in patients with Guillain-Barré syndrome. There is evidence that epitope recognition by molecular mimicry expands to multiple

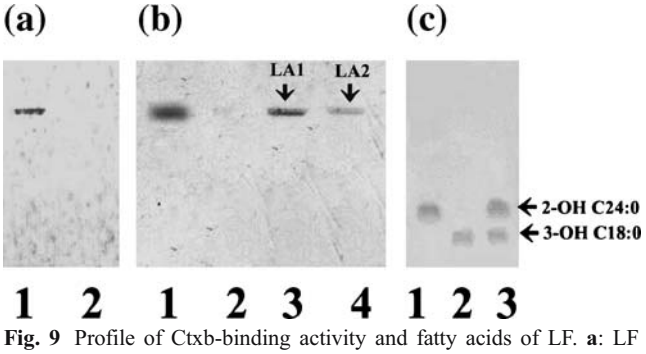

Fig. 9 Profile of Ctxb-binding activity and fatty acids of LF. **a**: LF was examined by TLC using the Dittmer staining before (lane 1) and after (lane 2) alkaline phosphatase treatment. **b**: LF was examined by TLC-overlay with Ctxb before (lane 1) and after (lane 2) alkaline phosphatase treatment. Authentic lipid A samples containing monophosphate (LA1) and diphosphates (LA2) were examined by TLC-overlay with Ctxb. **c**: Fatty acid methylester of LF was examined by TLC-iodine staining as described in "Materials and methods." Lane 1, authentic 2-hydroxy tetracosanoic acid methylester; 2, authentic 3-hydroxy octadecanoic acid methylester; 3, fatty acid methylester obtained after hydrolysis of LF

Table 2 Chemical composition of LF

MW 1836	mg	μmol	molar ratio
H_3PO_4 (Mw 98)	1.90	19.39	1.88
$GlcNH_2$-$GlcNH_2$ (Mw 372)	3.51	9.44	1.0
RCOOH (Mw 667)	14.01	21.00	2.22
Hexose	<0.1	–	–
Kdo	<0.1	–	–
Ethanolamine	<0.1	–	–

cross-reactivity (epitope spreading) [34]. Anti-GM1 antibody production in patients with GBS after an antecedent *C. jejuni* infection is associated with carbohydrate mimicry between the oligosaccharides of GM1 and LPS [9, 10]. Direct evidence has been provided by sensitizing Lewis rats with the LPS of *C. jejuni* HS 19, which results in the subsequent elevation of antibody titers against GM1 and GD3 in the sera of these animals [35]. Carbohydrate mimicry of the GD3 epitope has also been validated in the LPS fractions of *C. jejuni* (HS 19). In the present study, we found that the LOS extract of *C. jejuni* HS 19 cells consisted of two distinct molecules, LS and LF, that can be distinguished by TLC-overlay with Ctxb. To validate molecular mimicry between these components and GM1, we purified LS and LF and elucidated their chemical structures. From LS we obtained two oligosaccharides, one of which is a pentasaccharide and the other a trisaccharide. Structural analyses confirmed that LS is an octasaccharide containing a monophosphate group: Gal-GalNAc-(NeuAc) Gal-Hep-(Glc;PO_3H)Hep-Kdo. We could not obtain the native intact octasaccharide, probably because the native oligosaccharide could not survive the acid hydrolysis (1% acetic-acid hydrolysis for 1 h at 90°C), which would have cleaved the diheptose linkage. Nonetheless, we could validate the molecular mimicry for the tetrasaccharide remnant, Gal-GalNAc-(NeuAc)Gal, which is identical to that of the nonreducing terminal tetrasaccharide of GM1. This oligosaccharide residue clearly provides the structural basis for interaction with Ctxb. It should be mentioned that this terminal tetrasaccharide, Galβ1-3GalNAcβ1-4(NeuAcα2-3) Galβ1-4-with various degree of sialylation, has been previously reported in the LOS of HS 19 [36–38]. In the present study, we have further identified the same terminal core structure in strain HS 19 as the major component that is likely the antigenic epitope contributing to molecular mimicry in GBS.

On the other hand, we could not detect any GM1-like oligosaccharide epitope in LF. Instead, the LF was characterized as having a lipid A structure: 1, 4′-bisphosphoryl glucosamine-disaccharide *N, N'*-acylated by 3-(2-hydroxytetracosanoyloxy)octadecanoic acid at 2-and 2′-positions. The 3-hydoxyl group of the glucosamine-disaccharide of LF was not acylated by any fatty acids, presumably because of the elimination of any *O*-acyl group under that mild alkaline condition (25% ammonia for 48 h at 56°C). Consequently, the structure of LF was proposed to be the same as that shown in Fig. 8b. Although elimination of the *O*-acyl groups is expected to occur on the 3-(2-hydroxytetracosanoyloxy)octadecanoyl moiety, eventually the 2-hydroxytetracosanoyl group was retained in the proposed structure of LF. This finding also suggests the resistance of these ester-linked 2-hydroxyl fatty acids to mild alkaline hydrolysis [39].

Long-chain fatty acids such as 2-hydroxy tetracosanoic acid and 3-hydroxy octadecanoic acid are novel constituents to be seen in lipid A. These fatty acids have been found in lipid A of the *Agrobacterium* and *Mycobacterium*

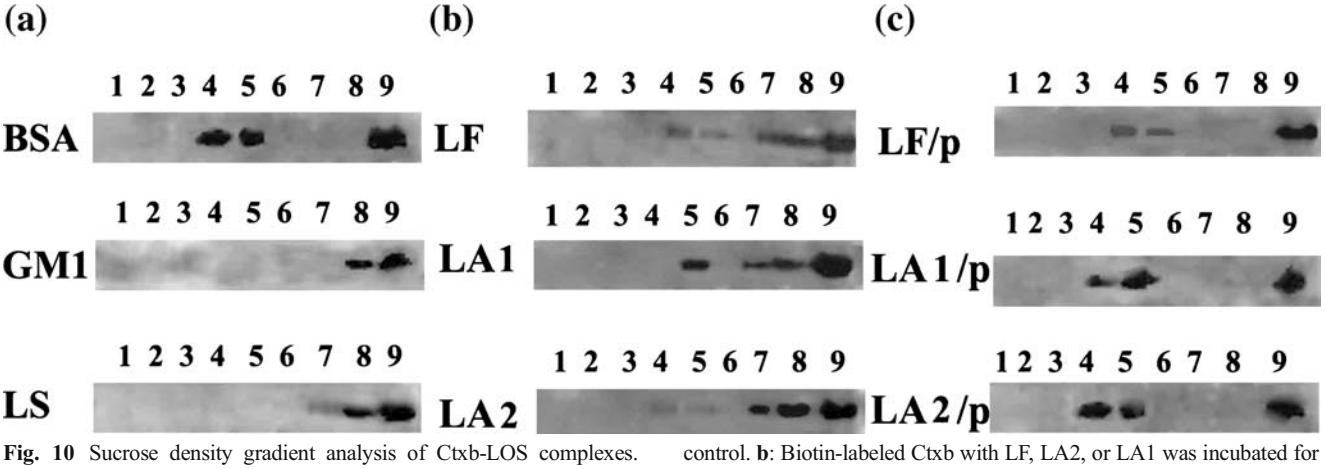

Fig. 10 Sucrose density gradient analysis of Ctxb-LOS complexes. **a**: Biotin-labeled Ctxb with BSA, GM1, or LS was incubated for 30 min and applied on the top of an 8–30% sucrose gradient and ultracentrifuged. Lanes 1–8 indicate blots of each fraction from top to bottom of the sucrose gradient; 9, biotin-labeled Ctxb as a positive control. **b**: Biotin-labeled Ctxb with LF, LA2, or LA1 was incubated for 30 min and subjected to blot analysis by the same protocol as above. **c**: Biotin-labeled Ctxb with LF/p, LA2/p or LA1/p obtained after phosphatase treatment of LF, LA2, or LA1, respectively, was incubated for 30 min and subjected to blot analysis by the same protocol as above

species [40, 41]. 2-Hydroxy tetracosanoic acid, also known as cerebronic acid, is abundant in the brain [42]. It is worth mentioning that subperineurial injections of very long-chain fatty acids into rat sciatic nerves caused demyelination [43]. If this were the case, there is an intriguing possibility that free fatty acids released from the LOS of infectious agents could also have pathogenic effects.

The interaction between LF and Ctxb is due to a mechanism that is entirely different from that of Ctxb with GM1 and LS. Analysis of complex formation between Ctxb and LF was examined by sucrose gradient centrifugation. We presumed that Ctxb-binding with LF is not restricted by the presence of specific long-chain fatty acids 3-(2-hydroxytetracosanoyloxy)octadecanoic acid because the Ctxb-binding activity was also seen in lipid A from *E. coli*, in which the Ctxb-binding activity seems to be independent of the fatty acid species of lipid A. Unexpectedly, 1, 4′-bisphosphorylation of the glucosamine moiety in the disaccharide structure of lipid A is essential for its interaction with Ctxb. Furthermore, the bisphosphorylated form is more active than the mono- and non-phosphorylated forms for Ctxb-lipid A complex formation, suggesting the possibility of an electrostatic interaction between the two components. Our data also point to the involvement of novel structures other than GSLs for interaction with Ctxb.

Recently, it has been reported that Kdo2-lipid A also possesses binding affinity to Ctxb to form a complex with LOS via a GM1-independent binding region [44]. The authors demonstrated that the phosphate group on the Kdo core of LOS from *Vibrio cholerae* as preventing Ctxb from binding to the LOS, resulting in the secretion of soluble toxin across the outer membrane. Our present investigation revealed that Ctxb had a novel binding site at the LF fraction (lipid A), in addition to the other site on the LS fraction (terminal tetrasaccharide with a GM1-like epitope). In contrast to the Kdo-lipid A core, the binding of Ctxb to lipid A apparently depends on the phosphorylation status of lipid A. Further studies are needed to elucidate the biological significance of this novel binding site.

Bacterial polysaccharides have been considered as classic *T* cell-independent antigens that do not facilitate cell-mediated immune responses [45]. However, it has been reported recently that the carbohydrate component of glycolipids and glycoproteins can influence T-cell responses [46]. Moreover, bacterial polysaccharides with a zwitterionic charge elicit a T-cell-dependent immune response [47]. These zwitterionic polysaccharides are processed to low-molecular weight carbohydrates by a nitro-oxide-mediated mechanism and presented to *T* cells through antigen presentation. These molecules are inactivated by chemical modification, which eliminates the charges of the carbohydrate moieties [48]. Although LF seems to be interactive with Ctxb by participation of the negatively charged phosphate moiety, LF might be further processed to a zwitterionic disaccharide by cleavage of the long-chain fatty acids and by binding to the major histocompatibility complex inside antigen-presenting cells for presentation to *T* cells [49]. Molecular mimicry as a mechanism of GBS is a complex phenomenon that also involves T-cell mediated immune response for the activation of autoreactrive *T* cells, and further studies are necessary for clarifying the immunopathogenic role of LF.

Acknowledgments This work was supported by an NIH grants NS-26994 to RKY and AI058284 to SAT. We thank Ms. Anke Beckedorf (Mass spectrometry/Proteomics Core Facility) for assistance in the mass-spectrometric analysis.

References

1. Kornberg, A.: Anti-GM1 ganglioside antibodies: their role in the diagnosis and pathogenesis of immune-mediated motor neuropathies. J. Clin. Neurosci. **7**, 191–194 (2000)
2. Arasaki, K., Kusunoki, S., Kudo, N., Tamaki, M.: The pattern of antiganglioside antibody reactivities producing myelinated nerve conduction block *in vitro*. J. Neurol. Sci. **161**, 163–168 (1998)
3. Hiraga, A., Kuwabara, S., Ogawara, K., Misawa, S., Kanesaka, T., Koga, M., Yuki, N., Hattori, T., Mori, M.: Patterns and serial changes in electrodiagnostic abnormalities of axonal Guillain-Barré syndrome. Neurology **64**, 856–860 (2005)
4. Ang, C.W., Jacobs, B.C., Laman, J.D.: The Guillain-Barré syndrome: a true case of molecular mimicry. Trends. Immunol. **25**, 61–66 (2004)
5. Willison, H.J.: The immunobiology of Guillain-Barré syndrome. J. Peripher Nerve. Syst. **10**, 94–112 (2005)
6. Ariga, T., Yu, R.K.: Antiglycolipid antibodies in Guillain-Barré syndrome and related diseases: review of clinical features and antibody specificities. J. Neurosci. Res. **80**, 1–17 (2005)
7. Raetz, C.R., Whitfield, C.: Lipopolysaccharide endotoxins. Ann. Rev. Biochem. **71**, 635–700 (2002)
8. Aleander, C., Rietschel, E.T.: Bacterial lipopolysaccharides and innate immunity. J. Endotoxin. Res. **7**, 167–202 (2001)
9. Allos, B.M., Lippy, F.T., Carlsen, A., Washburn, R.G., Blaser, M.J.: *Campylobacter jejuni* strains from patients with Guillain-Barré syndrome. Emerg. Infect. Dis. **4**, 263–268 (1998)
10. Nishimura, M., Nukina, M., Kuroki, S., Obayashi, H., Ohta, M., Ma, J.J., Saida, T., Uchiyama, T.: Characterization of *Campylobacter jejuni* isolates from patients with Guillain-Barré syndrome. J. Neurol. Sci. **153**, 91–99 (1997)
11. Kuziemko, G.M., Stroh, M., Stevens, R.C.: Cholera toxin binding affinity and specificity for gangliosides determined by surface plasma resonance. Biochemistry **35**, 6375–6384 (1996)
12. Morinaga, N., Iwamaru, Y., Yahiro, K., Tagashira, M., Moss, J., Noda, M.: Differential activities of plant polyphenols on the binding and internalization of cholera toxin in vero cells. J. Biol. Chem. **280**, 23303–23309 (2005)
13. Westphal, O., Luderitz, O., Bister, F.: Uber die Extraktion von Bakterien mit Phenol/Waser. Z. Naturforsch. **7b**, 148 (1952)
14. Usuki, S., Sanchez, J., Ariga, T., Utsunomiya, I., Taguchi, K., Rivner, M.H., Yu, R.K.: AIDP and CIDP having specific antibodies to the carbohydrate epitope (−NeuAcα2-8NeuAcα2-3Galβ1-4Glc-) of gangliosides. J. Neurol. Sci. **232**, 37–44 (2005)

15. Cameron-Smith, R., Harbour, C.: Removal of poliovirus type 1 from a protein mixture using an immunoaffinity chromatography column. Biomed. Chromatogr. **15**, 471–483 (2001)
16. Yoshimi, Y., Yamazaki, S., Ikekita, M.: Developmental changes in Asn-linked neutral oligosaccharides in murine cerebrum. Biochim. Biophys. Acta **1426**, 69–79 (1999)
17. Ito, M., Ikeda, K., Suzuki, Y., Tanaka, K., Saito, M.: An improved fluorescence high-performance liquid chromatography method for sialic acid determination: an internal standard method and its application to sialic acid analysis of human apolipoprotein E. Anal. Biochem. **300**, 260–266 (2002)
18. Fujii, T., Shimoi, H., Iimura, Y.: Structure of the glucan-binding sugar chain of Tip1p, a cell wall protein of *Saccharomyces cerevisiae.* Biochim. Biophys. Acta **1427**, 133–144 (1999)
19. Monsigny, M., Petit, C., Roche, A.C.: Colorimetric determination of neutral sugars by a resorcinol sulfuric micromethod. Anal. Biochem. **175**, 525–530 (1988)
20. Yasuno, S., Kokubo, K., Kamei, M.: New method of determining the sugar composition of glycoproteins, glycolipids, and oligosaccharide by high-performance liquid chromatography. Biosci. Biotechnol. Biochem. **63**, 1353–1359 (1999)
21. Murata, T., Shibatsuji, H., Yoshimi, Y., Hara, H., Yasuno, S., Yamaguchi, T., Moriya, H., Sweeley, C.C., Ikekita, M.: Structural characterization of sialylated and neutral N-linked oligosaccharides labeled with p-aminobenzoic acid octylester by high performance liquid chromatography and fast atom bombardment mass spectrometry. Res. Commun. Biochem. Cell. Mol. Biol. **1**, 285–303 (1997)
22. Drewry, D.T., Lomax, J.A., Gray, G.W., Wilkinson, S.G.: Studies of lipid A fractions from the lipopolysaccharides of *Pseudomonas aeruginosa* and *Pseudomonas alcaligenes.* Biochem. J. **133**, 563–572 (1973)
23. Aronson, N.N. Jr, Touster, O.: Isolation of rat liver plasma membrane fragments in isotonic sucrose. Methods Enzymol. **31**, 90–102 (1974)
24. Bartlett, G.R.: Colorimetric assay methods for free and phosphorylated glyceric acids. J. Biol. Chem. **234**, 467–471 (1959)
25. Reissig, J.L., Storminger, J.L., Leloir, L.F.: A modified colorimetric method for the estimation of N-acetylamino sugars. J. Biol. Chem. **217**, 959–966 (1955)
26. Dumcombe, W.G., Rising, T.J.: Quantitative extraction and determination of nonesterified fatty acids in plasma. J. Lipid. Res. **14**, 258–261 (1973)
27. Laemmli, U.K.: Cleavage of structural proteins during the assembly of the head of bacteriophage T4. Nature **227**, 680–685 (1970)
28. Ando, E., Terayama, H., Nishizawa, K., Yamakawa, T.: *Seikagaku Kenkyuho I* (Asakurashyoten, Tokyo, 1967), chapter 2, p.79
29. Wucherpfennig, K.W.: Structural basis of molecular mimicry. J. Autoimmun. **16**, 293–302 (2001)
30. Wucherpfennig, K.W.: Infectious triggers for inflammatory neurological diseases. Nat. Med. **8**, 455–457 (2002)
31. Cohen, I.R.: Principles of molecular mimicry and autoimmune diseases. In: Cummingham, M.W. (eds.) Molecular Mimicry, Microbes, and Autoimmunity, pp. 17–26. Fujinami RS ASM, Washington DC (2000)
32. Baum, H., Davies, H., Peakman, M.: Molecular mimicry in the MHC: hidden clues to autoimmunity. Immunol. Today **17**, 64–70 (1996)
33. Van Rhijn, I., Van den Berg, L.H., Ang, C.W., Admiraal, J., Logtenberg, T.: Expansion of human gammadelta T cells after *in vitro* stimulation with *Campylobacter jejuni*. Int. Immunol. **15**, 373–382 (2003)
34. Zhu, J., Pelidou, S.H., Deretzi, G., Levi, M., Mix, E., van der Meide, P., Winblad, B., Zou, L.P.: P0 glycoprotein peptides 56–71 and 180–199 dose-dependently induce acute and chronic experimental autoimmune neuritis Lewis rats associated with epitope spreading. J. Neuroimmunol. **114**, 99–106 (2001)
35. Usuki, S., Thompson, S.A., Rivner, M.H., Taguchi, K., Shibata, K., Ariga, T., Yu, R.K.: Molecular mimicry: sensitization of Lewis rats with *Campylobacter jejuni* lipopolysaccharides induces formation of antibody toward GD3 ganglioside. J. Neurosci. Res. **83**, 274–284 (2006)
36. Aspinall, G.O., McDonald, A.G., Raju, T.S., Pang, H., Mills, S. D., Kurjanczyk, L.A., Penner, J.L.: Serological diversity and chemical structures of *Campylobacter jejuni* low-molecular-weight lipopolysaccharides. J. Bacteriol. **174**, 1324–1332 (1992)
37. Aspinall, G.O., McDonald, A.G., Pang, H., Kurjanczyk, L.A., Penner, J.L.: Lipopolysaccharides of *Campylobacter jejuni* serotype O:19: structures of core oligosaccharide regions from the serostrain and two bacterial isolates from patients with Guillain-Barré syndrome. Biochemistry **33**, 241-249 (1994)
38. Yuki, N., Taki, T., Inagaki, F., Kasama, T., Takahashi, M., Sato, K., Handa, S., Miyatake, T.: A bacterium lipopolysaccharide that elicits Gullain-Barré syndrome has a GM1 ganglioside-like structure. J. Exp. Med. **178**, 1771–1775 (1993)
39. Silipo, A., Lanzetta, R., Amoresano, A., Parrilli, M., Molinaro, A.: Ammonium hydroxide hydrolysis: a valuable support in the MALDI-TOF mass spectrometry analysis of lipid a fatty acid distribution. J. Lipid. Res. **43**, 2188–2195 (2002)
40. Vilcheze, C., Morbidoni, H.R., Weisbrod, T.R., Iwsamoto, H., Kuo, M., Sacchettini, J.C., Jacobs, W.R., Jr.: Inactivation of the inhA-encoded fatty acid synthase II (FASII) enoyl-acy carrier protein reductase induces accumulation of the FASI end products and cell lysis of Mycobacterium smegmatis. J. Bacteriol. **182**, 4059–4067 (2000)
41. Silipo, A., De Castro, C., Lanzetta, R., Molinaro, A., Parrilli, M.: Full structural characterization of the lipid a components from the *Agrobacterium tumefaciens* strain C58 lipopolysaccharide fraction. Glycobiology **14**, 805–815 (2004)
42. Hoshi, M., Kishimoto, Y.: Synthesis of cerebronic acid from lignoceric acid by rat brain preparation. Some properties and distribution of the hydroxylation system. J. Biol. Chem. **248**, 4123–4130 (1973)
43. Sacktor, N.C., Griffin, J., Moser, A.B., Moser, H.W.: Effects of subperineurial injections of very-long-chain and medium-chain fatty acids into rat sciatic nerve. Neurochem. Pathol. **5**, 71–83 (1986)
44. Horstman, A.L., Bauman, S.J., Kuehn, M.J.: Lipopolysaccharide 3-deoxy-D-manno-octulosonic acid (Kdo) core determines bacterial association of secreted toxin. J. Biol. Chem. **279**, 8070–8075 (2004)
45. Abbas, A.K., Lichtman, A.H., Pober, J.S.: Cellular and Molecular Immunology chapter 9, pp. 209–210. WB Saunders, Philadelphia (1997)
46. Ishioka, G.Y., Lamont, A.G., Thomson, D., Bulbow, N., Gaeta, F. C., Sette, A., Grey, H.M.: MHC interaction and T cell recognition of carbohydrates and glycopeptides. J. Immunol. **148**, 2446–2451 (1992)
47. Kalka-Moll, W.M., Tzianabos, A.O., Bryant, P.W., Niemeyer, M., Ploegh, H.L., Kasper, D.L.: Zwitterionic polysaccharides stimulate T cells by MHC class II-dependent interactions. J. Immunol. **169**, 6149–6153 (2002)
48. Tzianabos, A.O., Onderdonk, A.B., Rosner, B., Cisneros, R.L., Kasper, D.L.: Structural features of polysaccharides that induce intra-abdominal abscesses. Science **262**, 416–419 (1993)
49. Cobb, B.A., Wang, Q., Tzianabos, A.O., Kasper, D.L.: Polysaccharide processing and presentation by the MHC II pathway. Cell **117**, 558–559 (2004)
50. Svennerholm, L.: The gangliosides. J. Lipid. Res. **5**, 145–155 (1964)